ELSEVIER

Marine Geology 186 (2002) 195–210

MARINE GEOLOGY
INTERNATIONAL JOURNAL OF MARINE GEOLOGY, GEOCHEMISTRY AND GEOPHYSICS

www.elsevier.com/locate/margeo

Experimental quasi-steady density currents

Jan Alexander [a,*], Thierry Mulder [b]

[a] School of Environmental Sciences, The University of East Anglia, Norwich NR4 7TJ, UK
[b] Département de Géologie et Océanographie, UMR 5805, Université Bordeaux I, Avenue des Facultés, 33405 Talence Cedex, France

Received 3 July 2001; accepted 17 April 2002

Abstract

Hyperpycnal flows may be important mechanisms for transporting particles from continents to oceans given their frequency of generation at many modern river mouths. Their deposits are probably very common in the rock record, although they are not frequently recorded in the literature. These currents may last longer and be steadier than surge-like turbidity flows and consequently their deposits are likely to be significantly different. In this paper simple laboratory experiments are used to investigate how flows and deposits may vary. The thickness of the experimental flows near the flow front varies with distance from the source depending on slope, effluent discharge, grain size and sorting. Runout distance varies with the proportion of fine-grained sediment rather than with mean grain size. Flow front velocity varies with effluent discharge and sediment concentration and in a complex manner with mean grain size and sorting. The variation of deposit mass with runout distance depends on proximal slope angle and the maximum mass per unit area (approximating to bed thickness) is inversely dependent on slope angle. Variation in initial suspended particle concentration results in deposits of similar shape but different volume. Although the total mass of the deposit depends on the discharge the maximum mass per unit area (approximating to maximum bed thickness) does not. The distance over which particles are deposited increases and the deposit flattens as particles are deposited progressively further downstream at higher discharges, perhaps relating to more efficient turbulent suspension at higher *Re* (more complete energy cascade), in addition to longer horizontal component of settling trajectory at higher velocity. The amplitude of mass variation depends on the grain size. As with laboratory surges [Gladstone et al., Sedimentology (1998) 833–844], the finer the sediment the more efficient is the sediment transport.

Keywords: tank experiment; hyperpycnal flows; turbidity currents; underflows

1. Introduction

Turbulent turbid river water can transform into a turbidity current when the concentration of suspended particles is such that the fluvial water density is greater than that of the water in the receiving basin. Such runoff-generated turbidity currents are commonly called hyperpycnal flows (Wright, 1977; Mulder and Syvitski, 1995; Mulder and Alexander, 2001a). Suspension-dominated hyperpycnal flows were first recorded in Lake Léman by Forel (1885, 1892) and are more common in lakes than in marine basins because lake water is generally less dense than seawater and consequently the amount of particles required to create

* Corresponding author. Fax: +44-1603-507719.
E-mail addresses: j.alexander@uea.ac.uk (J. Alexander), t.mulder@geocean.u-bordeaux.fr (T. Mulder).

0025-3227/02/$ – see front matter
PII: S0025-3227(02)00313-4

hyperpycnal flow is lower. However, more than 66% of the 230 rivers that Mulder and Syvitski (1995) analysed could produce turbulent underflows in marine basins directly from turbid river effluent during floods with a return period of 1000 years or less. Parsons et al. (2001) used laboratory experiments to demonstrate that sediment convection from hypopycnal plumes can generate secondary hyperpycnal flows at much lower sediment concentrations than considered by Mulder and Syvitski (1995). Kineke et al. (2000) described evidence for a divergent sediment plume (a hypopycnal plume and associated hyperpycnal flow) from the Sepik River, Papua New Guinea, which confirms the probable importance of these sediment dispersal mechanisms. Consequently hyperpycnal turbidity currents may be an important mechanism of sediment transport from continents to oceans. Given the frequency at which hyperpycnal flows are generated at the present day (cf. Mulder and Syvitski, 1995; Mulder et al., 2001b; Kineke et al., 2000) their deposits are probably very common in the rock record, although they are not frequently recorded in the literature.

Hyperpycnal flows can be maintained for a relatively long time (hours to months; cf. Mulder and Syvitski, 1995, 1996; Skene et al., 1997; Mulder et al., 1998) and the mean velocity at a site may be nearly constant over a prolonged period. Because of this they may be called quasi-steady currents and unlike surge-like flows (cf. Ravenne and Beghin, 1983; Mulder and Alexander, 2001a), it may not always be possible to distinguish a distinct head or tail. The steadiness of a turbidity flow has a major influence on deposit character (cf. Kneller, 1995). As hyperpycnal turbidity currents may have a longer duration and greater steadiness than surge-like flows their deposits are likely to be significantly different. Despite this they have not been reliably differentiated in the rock record. Few studies of hyperpycnal flows have been published (e.g. Hay, 1987; Normark, 1989; Chikita, 1990; Phillip and Smith, 1992) and few authors have suggested hyperpycnal turbidity currents as an explanation for observed deposits (e.g. Nemec, 1995; Syvitski and Schafer, 1996; Mulder et al., 1998, 2001a,b; Piper et al., 1999).

It is difficult to make observations within turbidity currents and particularly difficult to observe processes offshore from river mouths during large floods, when significant volumes of sand may be transported. The physical processes in major hyperpycnal currents consequently can only be related to their deposits through the use of analogues, numerical models and laboratory experiments (e.g. Middleton, 1993; Alexander, 1993; Kneller and Buckee, 2000). Laboratory experiments are useful for visualising patterns of behaviour even though there are considerable problems in comparing experiments directly with individual natural turbidity currents (Middleton, 1966, 1967; Ravenne and Beghin, 1983; Edwards, 1993; Kneller and Buckee, 2000). Natural currents vary greatly in size and duration such that any laboratory experiments may represent a subset of natural conditions. The primary advantage of laboratory experiments is that the influence of individual factors can be examined in isolation. This can only be achieved by experimental configurations that greatly simplify nature. Such simple experiments are valuable for understanding processes, but should only be compared with natural case studies with extreme care, particularly in the light of problems of scaling turbulent mixing (cf. Parsons and Garcia, 1998).

When river effluent reaches the sea, a large number of factors influence the fate of suspended sediment. These variables include: chemistry and temperature of the effluent and basin waters, suspended sediment concentration, grain size distribution, sediment composition, effluent discharge, channel and basin depth, offshore bathymetric slope, flow confinement (e.g. channels offshore), marine basin stratification, water surface elevation (e.g. storm surge), wave activity, and tidal currents. The relative importance of any of these to hyperpycnal turbidity current generation and behaviour is as yet unknown.

This paper presents the results of some highly simplified experiments that were designed in a provisional attempt to assess the influence of discharge, sediment concentration, proximal slope and grain sorting on the distribution of deposits of hyperpycnal flows.

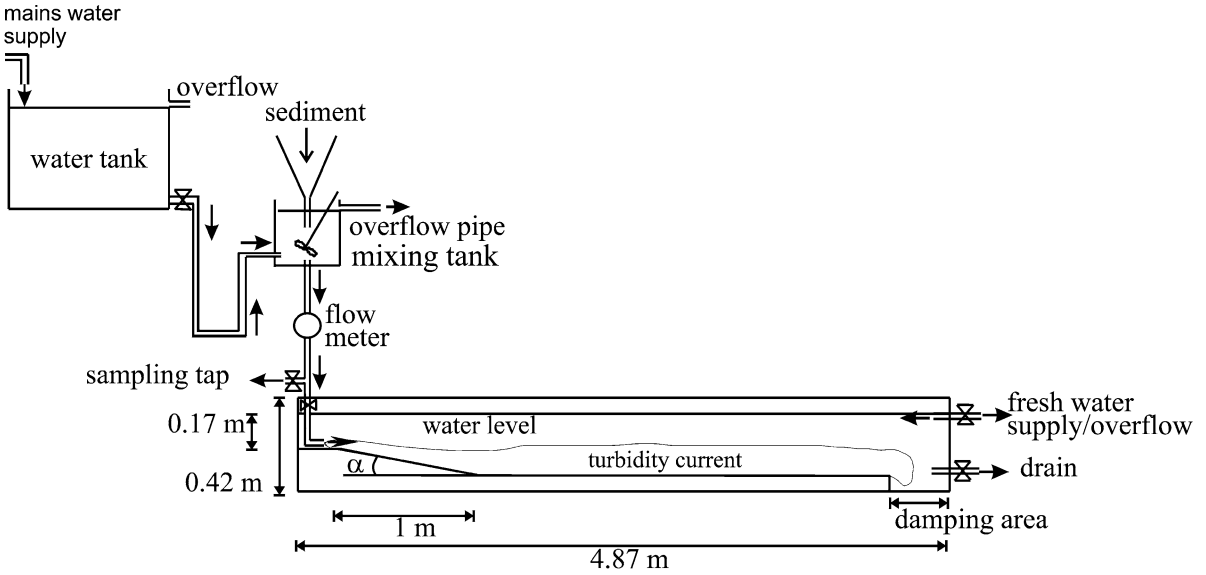

Fig. 1. Experimental tank configuration for quasi-steady density currents. The mouth of the input pipe rests on the false floor of the tank at the brink of the slope. The slope angle α was set at 0°, 3°, 6°, or 9° and the length of the slope was 1 m.

2. Introduction to the experiments

Twenty-four quasi-steady currents were produced in a transparent (perspex) tank (4.87 m long by 0.17 m wide and 0.52 m deep; Fig. 1; see Mulder and Alexander, 2001b for details on apparatus). Suspended sediment produced excess density for maintaining hyperpycnal flow. The discharge, suspended sediment concentrations, sediment grain size, sorting and bed slope were varied independently in successive runs (Table 1). Convection and lofting (cf. Sparks et al., 1993; Rimoldi et al., 1996) did not occur because of the absence of salt water. Consequently the experiments are especially relevant to lakes and in helping understanding the importance of processes in other settings.

The proximal slope of the experimental bed was varied at 3° increments from 0° to 9°. The 1 m long slope passed downstream onto a flat, horizontal platform, beyond which was a damping area designed to reduce volume and velocity of any reflected currents returning over the platform. The discharge was controlled by the difference in height between a header tank and experimental tank and thus the maximum discharge was limited by the height of the room.

Sediment was kept in suspension in the header tank by a propeller and the concentration of suspension was maintained by manual addition of water and sediment. The particle concentration of the flow entering the experimental tank was monitored by drawing off samples just above the pipe outlet (Fig. 1). Data presented here are from runs with discharges, Q_0, of 3.3×10^{-5}, 5×10^{-5} and 8.3×10^{-5} m^3 s^{-1} and particle concentrations of 5, 10 and 20 kg m^{-3}, corresponding to initial volumetric concentrations, C_0, of 0.23, 0.45 and 0.9%, respectively.

Four different grain sizes of silicon carbide (nominally 45, 63, 66 and 90 μm; Table 2) were used. This angular sediment is commercially available, easy to see, and allows direct comparison with published work on surge-like turbidity flow. At the start of each run it took about 2 s to attain the required discharge. When the effluent supply was turned off the flow quickly dissipated. The sediment settled in proximal areas of the tank such that none of the density currents reach the end of the tank.

Runs were recorded using a video camera (Sony CCD-TR2200E). The arrival time of the front of each flow at each 0.05 m mark (±5mm) down the length of the tank was mea-

Table 1
Experimental conditions for the runs used in this paper

Run No.	Laboratory No.	Slope	Input discharge ($\times 10^{-5}$ m^3 s^{-1})	Initial concentration (vol%)	Initial concentration (g/l)	Sediment nominal grain size (μm)	Input velocity at pipe mouth (m s^{-1})	Reynolds number at input point[a]	Froude number at input point
1	HP9601	9	8.33	0.9	20	45	0.265	5834	4.0341
9	HP9609	9	3.33	0.23	5	66	0.106	2331	3.2273
15	HP9615	3	5.00	0.45	10	45	0.159	3502	3.4231
17	HP9617	3	8.33	0.9	20	45	0.265	5834	4.0341
18	HP9618	3	8.33	0.9	20	90	0.265	5834	4.0341
19	HP9619	3	8.33	0.9	20	63	0.265	5834	4.0341
20	HP9620	3	8.33	0.9	20	66	0.265	5834	4.0341
22	HP9622	3	5.00	0.45	10	66	0.159	3502	3.4231
24	HP9624	3	5.00	0.45	10	66	0.159	3502	3.4231
25	HP9625	3	3.33	0.23	5	66	0.106	2331	3.2273
30	HP9630	6	8.33	0.9	20	66	0.265	5834	4.0341
44	HP9644	6	5.00	0.45	10	66	0.159	3502	3.4231
45	HP9645	9	5.00	0.45	10	66	0.159	3502	3.4231
46	HP9646	0	5.00	0.45	10	66	0.159	3502	3.4231
47	HP9647	0	3.33	0.23	5	66	0.106	2331	3.2273
49	HP9649	0	8.33	0.9	20	66	0.265	5834	4.0341
50	HP9650	0	5.00	0.45	10	66	0.159	3502	3.4231
51	HP9651	0	3.33	0.23	5	66	0.106	2331	3.2273
52	HP9652	9	5.00	0.9	20	45	0.159	3502	2.4205
53	HP9653	9	3.33	0.9	20	45	0.106	2331	1.6137
54	HP9654	9	5.00	0.45	10	45	0.159	3502	3.4231

N.B. The duration of all the runs reported here was 600 s.
[a] Assuming kinematic viscosity close to the viscosity of fresh water (10^{-6} m^2 s^{-1}).

sured with a 1/25 s accuracy from the video record. The flow front thickness (±5 mm), defined as the maximum thickness measured over the leading 0.25 m of the flow behind the front, was measured as the flow front reached each 0.05 m mark. It was more difficult to measure the flow front arrival times when the front was not perpendicular to the tank side over the full width (nota-

Table 2
Characteristics of the sediment used in the experiments

	Fine-grained SiC	Medium-grained SiC	Coarse-grained SiC	Equal mixture of three samples of SiC
Nominal grain size (1-ϕ range retained on nominal grain-size sieve) (μm)	45	63	90	66
Mean equivalent spherical diameter from Sedigraph (μm)	38.3	56.8	78.8	58
Standard deviation	11.8	17.9	24.0	
Grain shape	very angular low sphericity	very angular low sphericity	very angular low sphericity	very angular low sphericity
Skewness	0.28	0.212	0.186	
Kurtosis	0.79	0.83	0.51	
Mean settling velocity (m s^{-1}) from 20 unhindered settling experiments		4.88×10^{-3}	8.84×10^{-3}	
Density (kg m^{-3})	3220	3220	3220	3220

ble near the pipe outlet where the flow expanded laterally) or where the flow front was diffuse, near the distal end of the flow.

Sediment mass measurements are probably the most accurate measure of deposit distribution because thickness varies with fabric and newly deposited sediment consolidates rapidly. To measure deposit mass distribution a siphon tube was used to collect all sediment from 0.05×0.17 m areas of the tank floor, at intervals along the tank. Accurate delimitation of sampling rectangles was difficult, as a siphon tube or any other tool to delimit rectangles induced remobilisation of the fine-grained sediment that could pass from one sampling area to another, introducing an error of perhaps as much as 13% in extreme cases. As most of the error in sampling results from remobilisation of sediment between adjacent sample areas, a continual sampling pattern was used to assess the mass distribution. Each mass sample was filtered and dried before weighing (± 0.002 g).

Grain size samples were collected using a syringe from up to 10 sites with sampling interval increasing with distance down the tank, and these samples were analysed using a Sedigraph.

2.1. Scaling and similarity to natural flow conditions

Flow behaviour observed in the laboratory may be related to the behaviour of much larger natural currents via the scaling laws for hydraulic phenomena (e.g. Reynolds–Froude modelling). The flows can be described using the non-dimensional Froude, Richardson and Reynolds numbers. The densimetric Froude number, Fr, is given by:

$$Fr = \frac{V}{\sqrt{g h_b \cos \alpha \frac{\rho_f - \rho_a}{\rho_a}}} \quad (1)$$

where ρ_f is the bulk density of the flow, ρ_a is the ambient water density, h_b is the height of the flow body, g is the acceleration due to gravity, α is the bed slope and V is the mean forward velocity. Although very few natural hyperpycnal flows have been instrumented, it is likely that parts of some flows are supercritical ($Fr > 1$) while others are subcritical ($Fr < 1$) (cf. Garcia, 1993; Morris et al., 1998). Underflows monitored in the Katsurozawa Reservoir had densiometric Froude numbers of 0.545–0.876 (Chikita, 1990). The experimental flows were supercritical at the pipe mouth, but became subcritical within decimetres.

The Bulk Richardson number, Ri:

$$Ri = \frac{g(\rho_f - \rho_a) h_b \cos \alpha}{V^2 \rho_a} \quad (2)$$

is used to assess the stability of the flow boundaries (cf. Fukushima et al., 1985; Parker et al., 1986). Kelvin–Helmholtz instability usually develops when Ri is less than 0.25 (Simpson, 1987). The 'local-gradient' Richardson number, Ri_g, which concerns the stability of the interface itself, however, may be more important for mixing than the bulk Richardson number. Data on Ri and Ri_g for natural flows have not been published nor have reliable observations of the nature of flow boundaries.

The Reynolds number, Re:

$$Re = Vh/\mu \quad (3)$$

where μ is the apparent kinematic viscosity, delineates laminar ($Re < 500$), transitional ($500 < Re < 2000$) and turbulent ($Re > 2000$) flow. Parsons and Garcia (1998) and others show that mixing between the ambient fluid and the gravity current's head is dependent on Reynolds number with transition at $Re \sim 2 \times 10^5$ such that below about that value runout and deposit distribution depend on Reynolds number. Underflows monitored in the Katsurozawa Reservoir had $Re = 0.96\text{–}3.59 \times 10^5$ (Chikita, 1990), whereas underflows in the Queens Inlet, Alaska, (Phillip and Smith, 1992) had $Re = 1.4 \times 10^6$. Both of these examples are relatively small and velocity and flow thickness in other settings could be much greater (range of m s^{-1}; e.g. Piper and Savoye, 1993), such that the Re may be much greater. The laboratory flows were turbulent over much of the runout distance and consequently superficially comparable to smaller natural flows. However, Re is in the range where the mixing at the flow front

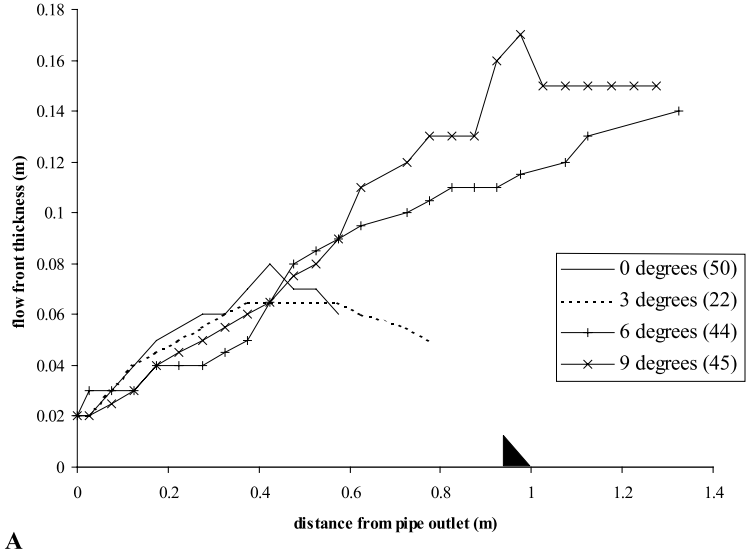

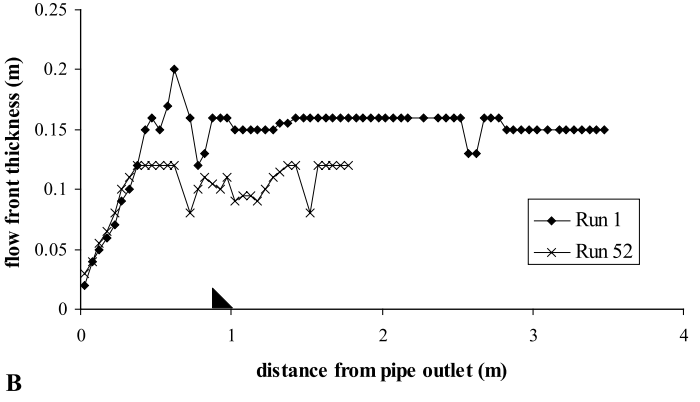

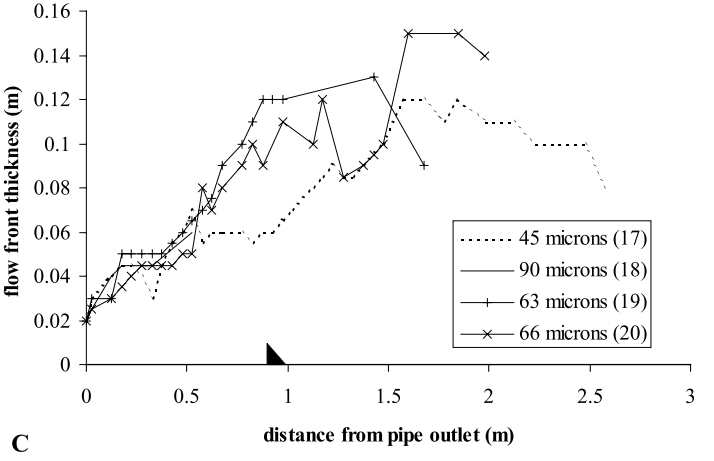

Fig. 2. The thickness of the flow front defined as the maximum thickness measured over the leading 0.25 m of the flow. (A) Comparing runs with different proximal bed slope (0°, 3°, 6° and 9°) but constant initial concentration (0.45%), discharge (5×10^{-5} m^3 s^{-1}) and grain size (nominally 66 μm). Run numbers are in brackets. The solid triangle marks the position of the end of the slope. (B) Comparing runs with different discharges, but constant proximal bed slope (9°), initial concentration (0.9%), and grain size (nominally 45 μm). Discharge of Run 1 was 8.33×10^{-5} m^3 s^{-1} and Run 52 was 5.00×10^{-5} m^3 s^{-1}. (C) Comparing runs with differing grain sizes (nominally 45, 63, 66 and 90 μm) but the same initial concentration (0.9%), discharge (8.33×10^{-5} m^3 s^{-1}), and bed slope (3°). Run numbers are in brackets.

will relate to *Re* (cf. Parsons and Garcia, 1998) and is never as high as is likely to be the case in many larger natural flows. Thus mixing in our flow is not scaled properly but the bulk deposits will be qualitatively similar to natural deposits.

Depending on the temperature and salinity of the basin water, river effluent must have more than 36–44 kg m^{-3} of suspended sediment to produce a hyperpycnal flow (Mulder and Syvitski, 1995); this corresponds to a 1.36–1.66% minimum volumetric concentration (assuming the particles have density of quartz). Most natural hyperpycnal currents will have volumetric concentrations well below 9% except at the base where bedload dominates (Mulder and Syvitski, 1995). The experiments used fresh water throughout so that equivalent density contrasts need much lower sediment concentrations (0.23, 0.45 and 0.9% initial concentrations used here).

In natural currents fine sand, silt and clay can be transported over long distances before being deposited. The river effluent velocity may be a few m s^{-1} during peak runoff. The velocity at the laboratory pipe outlet cannot exceed a couple of tens of cm s^{-1}, and most of the sediment must settle to the bed before the flow reaches the tank end-wall to prevent ponding and flow reversals. This restricts the sediment to coarse silt or sand, i.e. a similar size range to many natural flows. Given the sediment size and the bulk flow characteristics (cosmetically turbulent but possibly lacking the full range of scales necessary to maintain a turbulent cascade), it is likely that the laboratory currents have Stokesian settling and sorting, while in nature, vortex shedding from particles will be important. Because of these technical restrictions, the experimental currents behave intermediately between bedload-dominated flows, involving coarse particles that settle close to the river mouth and suspension-dominated hyperpycnal flows. The experiments are models for currents transporting coarse (sand grade) or dense sediment and relatively little fine-grained or low-density sediment.

In shallow water experiments, the ambient water above the flow may be active such that return flow is important (Huppert and Simpson, 1980). When the water is very shallow, return flow of water above the current may limit water entrainment into the flow and restrict flow velocity. Experiments with a sloping bed need a deep tank to reduce friction on the upper surface of the flow and the impact of reverse flows on the flow behaviour. Apart from the most proximal area on the slope, flow thickness never exceeds half the total water depth.

3. Results

3.1. Visual observations of flow behaviour

Each run produced a distinct flow front that moved steadily along the tank. Unlike surge-like flows that produce a distinct head and body (Laval et al., 1988; Ravenne and Beghin, 1983) it was not easy to define a distinct head in these flows. There were no obvious billows behind the flow front. De Rooij and Dalziel (2001) described a similar lack of distinct head in a quasi-steady flow experiment. All of the runs, over much of their runout, are strongly depletive (decreasing velocity with distance, cf. Kneller, 1995).

In all runs the thickness of the flow front increased rapidly in a similar manner over the proximal c. 0.2 m, but beyond that the thickness change depended on slope angle, discharge, initial concentrations and sediment grain size (Fig. 2). The velocity of the effluent at the pipe outlet, V_0, was calculated using:

$$V_0 = Q_0/\pi r^2 \quad (4)$$

where r is the internal radius of the pipe and Q_0 discharge. In a few runs the recorded velocity of the flow front increased a little above V_0 in very proximal areas (Fig. 3). Flow front velocity dropped rapidly from a point at or near (c. 0.1 m) the pipe outlet and then decreased exponentially with distance. The most proximal behaviour is governed by expansion from the pipe.

Runs with different bed slopes suggest that the patterns of flow thickness and velocity may be insignificantly different on gentle slopes (Figs. 2A and 3A). In runs with 0° and 3° proximal

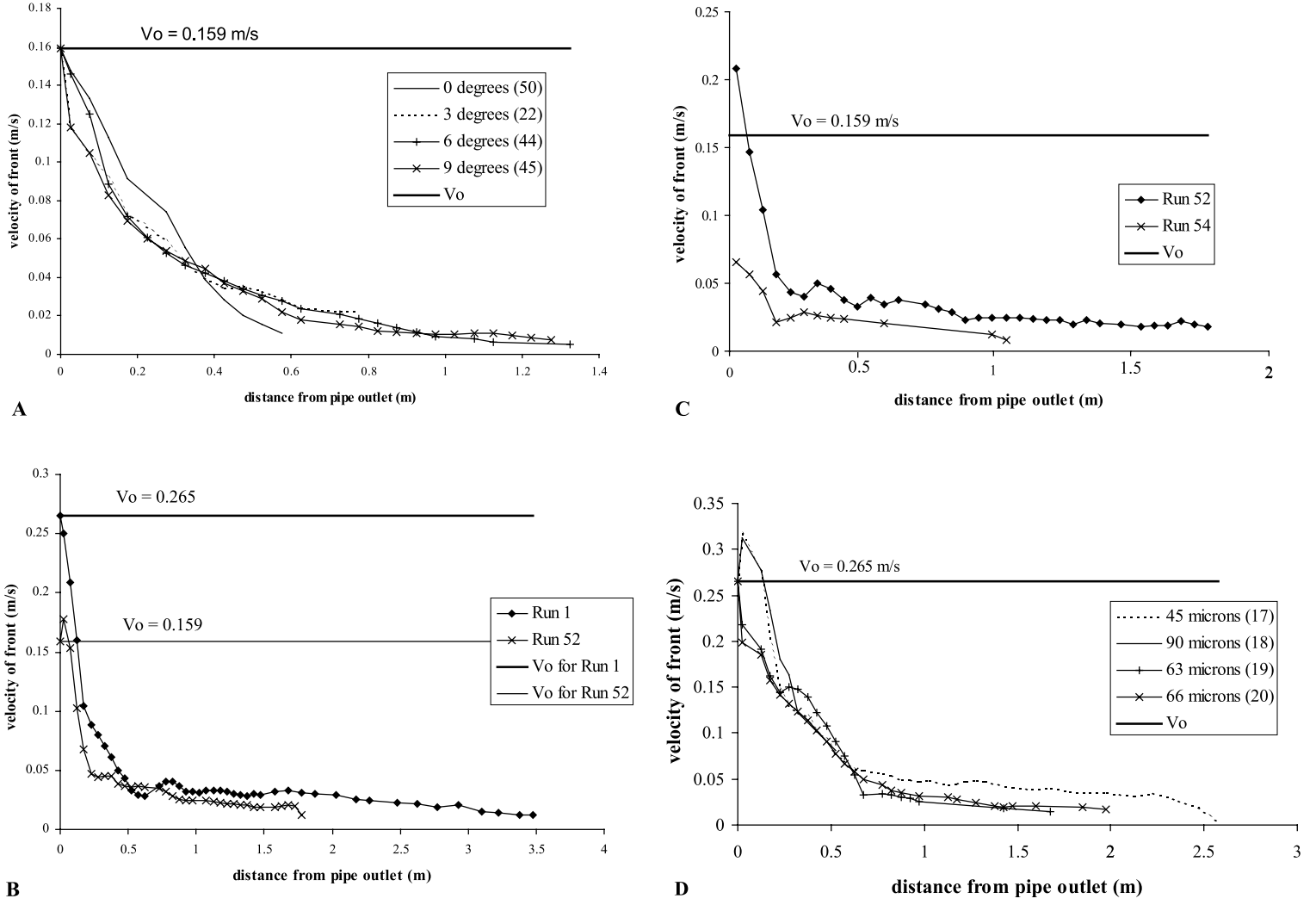

Fig. 3. Flow front velocities. The calculated outlet velocities ($V_0 = Q/\pi r^2$) are represented by horizontal lines, and in runs with a sloping bed, the slope terminated at 1 m from the pipe outlet. (A) Front velocities of runs with different proximal bed slope (0°, 3°, 6° and 9°) but constant initial concentration (0.45%), discharge (5×10^{-5} m^3 s^{-1}) and grain size (nominally 66 μm). Run numbers are in brackets. (B) Comparing runs with different effluent discharges (8.33×10^{-5} and 5×10^{-5} m^3 s^{-1}), but constant bed slope (9°), initial concentration (0.9%), and grain size (nominally 45 μm). (C) Comparing front velocities of runs with different initial sediment concentrations (0.45% and 0.9%), but constant discharge (5×10^{-5} m^3 s^{-1}), bed slope (9°), and grain size (nominally 45 μm). (D) Comparing runs with differing grain sizes (nominally 45, 63, 66 and 90 μm) but the same initial concentration (0.9%), discharge (8.33×10^{-5} m^3 s^{-1}), and bed slope (3°).

bed slope, beyond about 0.5 m the thickness stayed approximately constant or declined gradually until the flow was too dilute for the thickness to be defined with confidence. With greater slope, however, thickness expansion continued (Fig. 3A), as has been observed also in surge-like flows (Middleton, 1966; Mulder and Alexander, 2001b). The steeper the slope in the proximal area, the greater the distance over which the flow remained identifiable on the flat distal surface.

Beyond the proximal c. 0.2 m, the flow thickness depends on discharge. The greater the discharge the thicker the flow becomes and the further it travels (compare two runs with identical conditions other than discharge, Fig. 2B). Flows with greater discharge, and therefore higher pipe effluent velocity, maintain higher velocity for greater distances from the pipe outlet (Fig. 3B).

Figs. 2C and 3D show how the flow front thickness and velocity evolve in four flows transporting differing grain sizes. In proximal areas (less than c. 0.75 m) the thickness behaviour is indistinguishable (within the errors of thickness measurement) but the velocity varied quite a lot. This variation cannot be related to sediment grain size in any simple way and may reflect minor variations in the laboratory conditions. In more distal areas the flow behaviour depends on grain size and sorting. In the run that transported coarse fraction only most of the sediment had been deposited in the proximal 0.7 m and the flow could not be observed beyond that point. The flows with 63 and 66 μm sediment became thicker in more proximal sites than the flow with 45 μm sediment. Although the mean grain size of the 63 and 66 μm flows was very similar the flow which contained a higher proportion of fine-grained sediment (the 66 μm nominal flow) could be recognised as a flow further along the tank (Fig. 2B). The flow with the finest particles maintained higher velocity for longer than all other flows. Runout distance varied with the proportion of fine-grained sediment rather than with mean grain size. With the two flows with similar mean grain size the more poorly sorted flow maintained higher velocity for longer. This is comparable to the patterns of flow efficiency observed in surge-like gravity currents by Gladstone et al. (1998).

Flows with different initial suspended sediment concentrations behave very differently (Fig. 3C) as, beyond the pipe, the flow behaviour is governed by the density contrast between the flow and ambient water, which is controlled by the sediment load. Lower-concentration flows decelerate very rapidly, have shorter runout and are slower throughout their travel history. We do not have many data on flows with differing initial concentrations, but qualitative comparison suggests that if all else is constant then lower-concentration flows are thinner and travel less far.

To assess the internal steadiness an attempt was made to measure velocity within the flow, by observing individual particles or pulses of slightly more concentrated fluid (caused by sampling from input pipe, Fig. 4B). Internal velocity measurement was difficult and required chance observations on video records. In some cases velocity decreased after passage of the front then stabilised or rose slightly. Fig. 4A shows an example where velocity in the proximal 0.21 m declined fractionally after passage of the flow front, while at intermediate distances the internal velocity was a little higher than the front velocity. Acoustic Doppler velocimeters allow more accurate assessment of flow structure in experiments but this equipment was not available.

3.2. Discussion of flow characteristics

In the most proximal area the effluent behaves as a jet and flow spreads from the pipe to the full width of the tank evolving into a negatively buoyant plume. This transition is not accounted for in the Reynolds–Froude model and the most proximal data points (within the first 20–30 cm) may best be ignored. This proximal area, however, may be taken as a simple representation of a turbidity current exiting a canyon. Imran et al. (1998) modelled the behaviour of turbidity currents freely speeding after exiting a canyon and found a tendency for channel inception resulting from the lateral variation in distribution of erosion and deposition. The resulting geometry is somewhat similar to our experiments in which there is some initial lateral spread before the current is confined by the tank walls which approx-

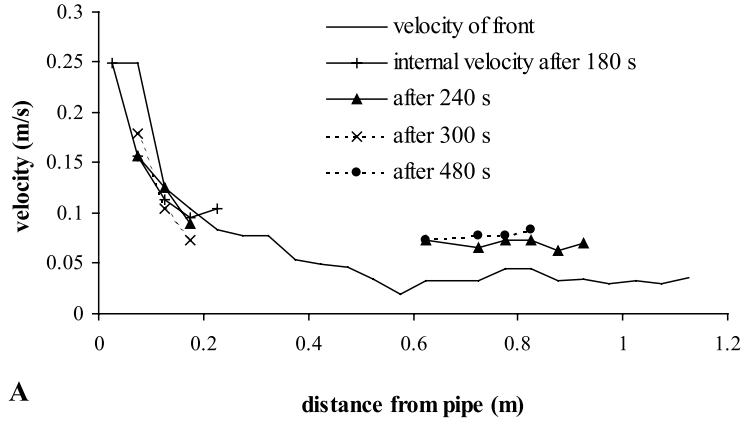

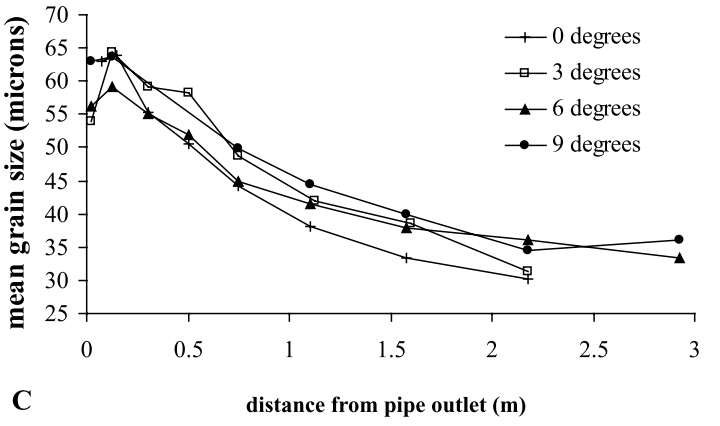

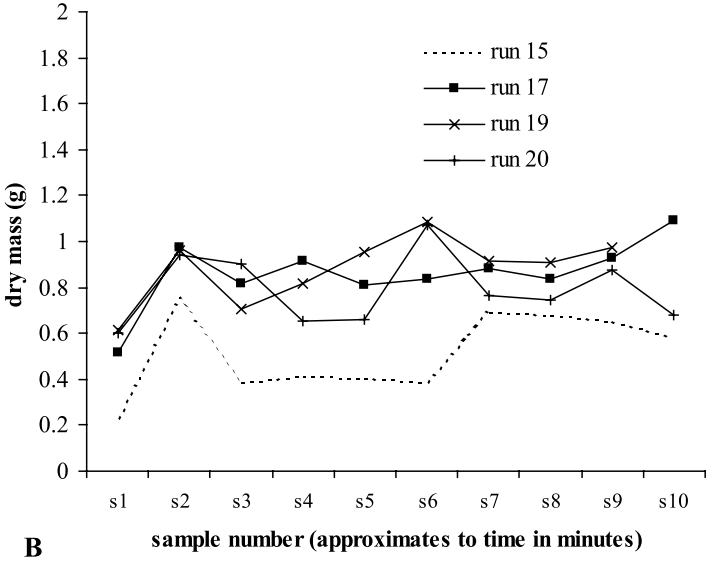

Fig. 4. (A) Comparison of flow front velocities and internal velocities in Run 1 (slope = 9°, discharge = 8.33×10^{-5} m^3 s^{-1}, initial concentration = 0.9%, grain size = 45 μm). The internal velocities measured 180, 240, 300 and 480 s after passage of the flow front were fractionally lower than the front velocities in the most proximal areas (< 0.22 m) but at intermediate distances were slightly higher. (B) Dry mass of samples draw off at intervals through experiment runs. Samples were taken at approximately minute intervals. Run 15 had a lower discharge and initial concentration than the other runs presented in this graph. (C) Variation in mean grain size with distance for runs on differing proximal slopes (Runs 49, 20, 30 and 37b).

imate to the channel developed in the Imran et al. (1998) model.

The water entrainment rate is directly related to the increase in flow thickness (Ellison and Turner, 1959). The high entrainment rate in proximal areas of these experimental currents relates to unstable flow interfaces (i.e. low Richardson number, *Ri*). But at some distance from the outlet the flows maintain constant thickness or decline in thickness suggesting that fluid entrainment becomes negligible.

The kinematic viscosity of the flow must vary continuously with position and time as the sediment concentration changes. For very dilute flows, kinematic viscosity is close to that of fresh water (10^{-6} m^2 s^{-1}), providing a limiting value for Reynolds number calculations. The flow front areas are cosmetically fully turbulent over much of the travel path for $C_0 = 0.9\%$ and high discharge values except in the most distal areas (Fig. 5). Most of the flows with $C_0 = 0.45\%$ become transitional beyond about 0.5 m (Fig. 5). Whatever the estimated viscosity, results demonstrate the difficulty in creating fully turbulent flow in the laboratory in particular because of the limits on flow thickness. A serious consequence of this is that the deposition patterns in part relate to the turbulence intensity. In addition, in natural flows vortex shedding from transported particles may be more important than in these experiments.

3.3. The deposits mass distribution and grain size

Near the pipe outlet, the deposit mass increases over a short distance depending on the discharge (up to 0.3 m) as a result of the deceleration associated with flow spreading from the pipe to the full width of the tank. This represents an area where the experiment is not 2D; however, most equivalent natural settings are also sites where flow can spread laterally. The deposits were 0.02–0.04 m thick in the proximal areas (0.075–0.3 m) with thickness varying across the tank. The maximum deposited mass corresponds with the site of rapid velocity decrease. Beyond the peak, the mass decreases exponentially. A similar exponential decrease with distance was observed in the experiment described by De Rooij and Dalziel (2001).

Runs with different proximal slopes had a small variation in the total deposited mass that could have resulted from a combination of (a) sampling errors, (b) error in initial concentration or fluctuations in concentration, or (c) slight variations in run duration. To allow better comparison between these runs the mass was normalised by dividing each sample mass by the total sample mass for that run (Fig. 6A,B). This confirmed an intuitively obvious mass distribution with runout distance depending on slope angle and maximum thickness inversely dependent on slope angle.

Three runs with different discharges demonstrate the variation in deposit mass distribution with discharge (Fig. 6C). As is intuitively obvious the total mass distribution of the deposit depends directly on the discharge. The maximum of mass per unit area (thickness), however, does not. The distance over which particles are deposited increases, and the deposit flattens, as particles are deposited progressively further downstream at higher discharges, perhaps relating to more efficient turbulent suspension at higher *Re* (more complete energy cascade), in addition to a longer horizontal component of settling trajectory at higher velocity.

Runs with differing initial concentrations show that the increase in suspended particle concentration results in deposits of similar shape but different maximum mass per unit area (Fig. 6D). The total mass deposited increases with initial sediment concentration and the distance over which sediment is transported also increases.

In the four runs with differing sediment grain sizes there was some variation in total sampled mass between runs so that the data were normalised to total run mass (Fig. 6E). The position of the mass peak was very similar in all four runs but its amplitude depended on grain size. The finer the grain size the more sediment was deposited further from the pipe outlet (Fig. 6E), in a pattern comparable to that observed by Gladstone et al. (1998) for surges.

It would be an oversimplification to assume constant sediment flux to the bed at any point

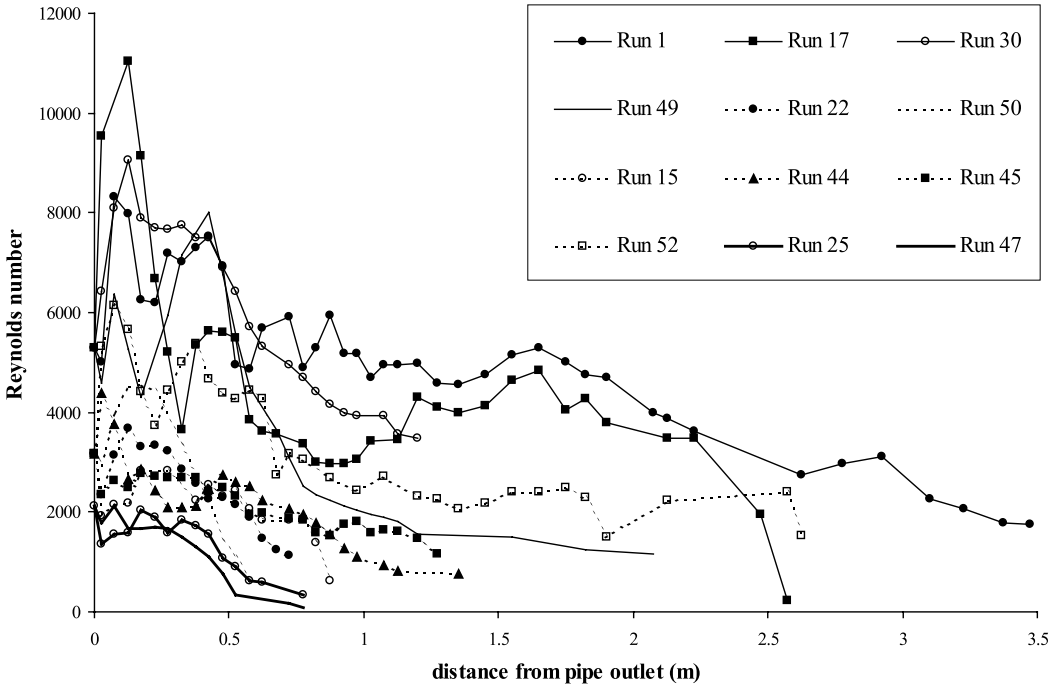

Fig. 5. Graph of Reynolds numbers calculated for representative experimental runs. The thin solid lines are runs with discharge of 8.33×10^{-5} m^3 s^{-1}, the dashed lines 5×10^{-5} m^3 s^{-1} and the thicker solid lines 3.33×10^{-5} m^3 s^{-1}. The lines with no symbol are for runs with 0° proximal slope, circles for 3°, triangles for 6° and squares for 9°.

throughout the duration of the run as the whole of the flow is not steady while the flow front travels down the tank (thus the use of quasi-steady in the paper's title). De Rooij and Dalziel (2001) document a change in sediment flux with time in the their shorter-duration experiments related to passage of the flow front.

The deposits' mean grain size gently decreases with distance from the pipe outlet (Fig. 4C). Mean grain size declines exponentially with distance. The data for equivalent runs on different proximal slopes suggest that there is a displacement of the curve with slope, but the sampling errors and grain size analysis make accurate assessment of this variation difficult.

4. Quasi-steady hyperpycnal turbidity currents and surge-like flows

During flood discharge, suspended sediment load is transported basinward through hyperpycnal, mesopycnal, homopycnal or hypopycnal plumes (depending on suspended sediment concentration and receiving basin characteristics: Mulder and Alexander, 2001a,b). In any eventuality, large quantities of sediment may be dumped at or near the river mouth, considerably increasing the local sedimentation rate. Shallow sediment failures can then occur, transforming quickly into surge-like sediment-driven flows such as those recorded in the fjords of British Columbia (Bornhold et al., 1994) and in the Var Canyon (Gennesseaux et al., 1971; Mulder et al., 1996). Consequently surge-like and hyperpycnal quasi-steady flows may occur simultaneously in the same area (possibly interacting) and it may be unlikely that hyperpycnal turbidites could be found in sites where deposits of surge-like flows do not also occur.

Surge-like flows may be catastrophic and are unsteady phenomena exhibiting a very wide range of sediment concentrations from $>45\%$ to below 9% (see Mulder and Alexander, 2001a). In con-

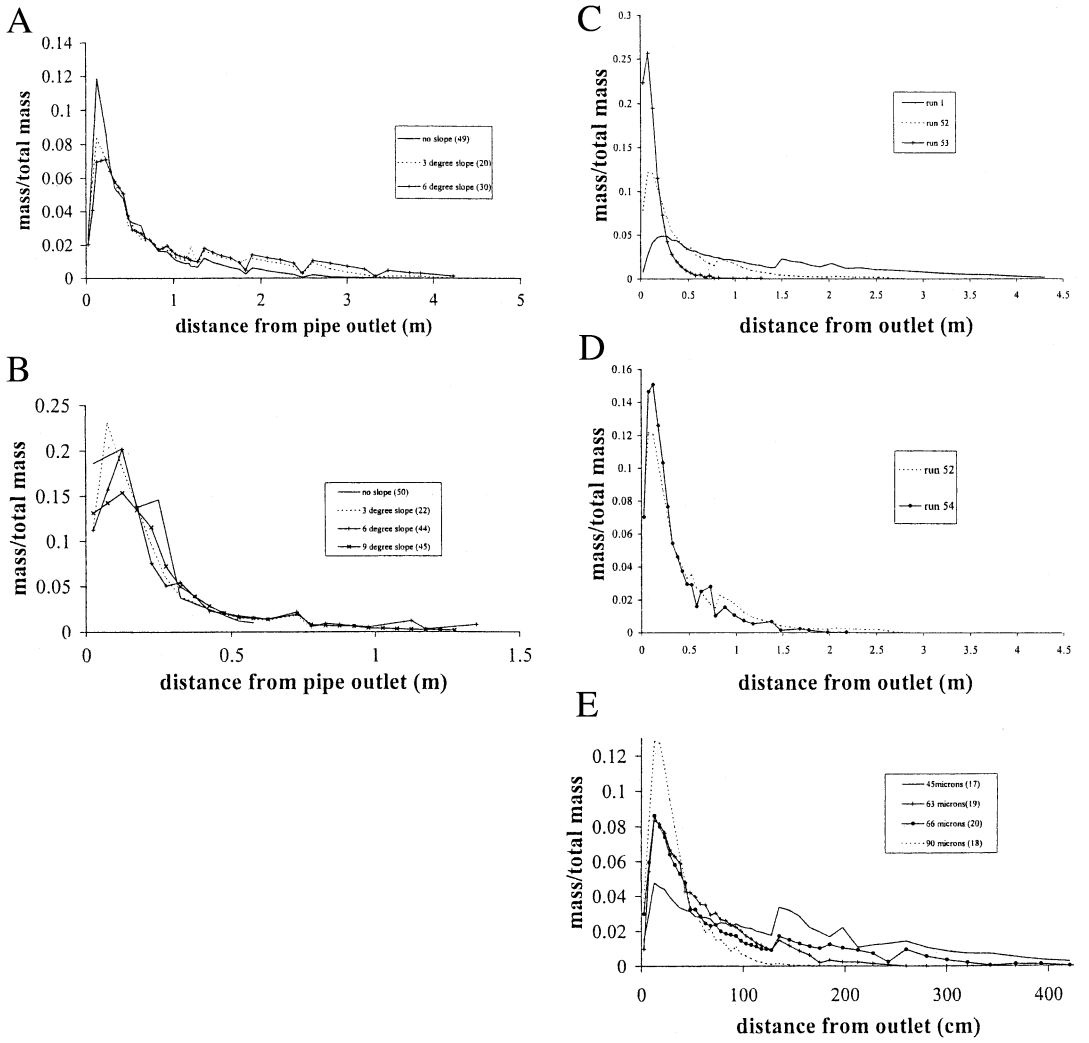

Fig. 6. Graphs to show deposit mass distribution. The sample mass data are presented as a fraction of the total mass of deposit to make comparison between runs with different total masses easier. (A) Mass distribution from runs on different slopes but with all other conditions constant ($Q = 8.3 \times 10^{-5}$ m^3 s^{-1}; nominal grain size = 66 μm; initial concentration = 0.9%. Run numbers are in brackets. (B) Mass distribution from runs on different slopes but with all other conditions constant ($Q = 5 \times 10^{-5}$ m^3 s^{-1}; nominal grain size = 66 μm; initial concentration = 0.45%. Run numbers are in brackets. (C) Mass distribution from runs with different discharges but with all other conditions constant (nominal grain size = 45 μm; initial concentration = 0.9%, slope = 9°). Discharges or Run 1 was 8.3×10^{-5} m^3 s^{-1}, Run 52 was 5×10^{-5} m^3 s^{-1} and Run 53 was 3.3×10^{-5} m^3 s^{-1}. (D) Mass distribution from runs with different initial suspended sediment concentrations but with all other conditions constant (nominal grain size = 45 μm; discharge = 5×10^{-5} m^3 s^{-1}, slope = 9°). The initial concentration in Run 52 was 0.9% and in Run 54 it was 0.45%. (E) Mass distribution from runs with different grain sizes (45, 63, 66 and 90 μm) but with all other conditions constant (discharge = 8.3×10^{-5} m^3 s^{-1}, slope = 3°; initial concentration = 0.9%). Run numbers are in brackets.

trast, suspended loads exceeding 230 kg m^{-3} are very infrequent at river mouths and only occur in unusual settings, such as after collapse of muddy river banks associated with heavy rainfall (e.g. in the Var; Laurent, 1971), in Chinese rivers eroding loess (Mulder and Syvitski, 1995; Xu, 1999), or when lahars or jökulhlaups reach the sea (e.g. Russell and Knudsen, 1999). Turbidity currents

generated directly from high suspended sediment load in rivers will tend to be dominated by particles finer than medium sand, whereas surge-like flows, because of their potentially greater density (and therefore velocity) may transport coarser sediment.

Surge-like flows generated from slope failure undergo a period of acceleration to a maximum velocity (as do lock-exchange experiments), whereas quasi-steady flows (both natural and in the laboratory) have momentum on entering the basin. This momentum difference probably accounts for much of the difference in deposit variation with distance in flows of similar concentration and volume. Along the travel path of either type of flow, beyond any area of significant erosion (after any ignition) the density of the flow and the sediment concentration both decrease because of ambient water entrainment and deposition.

In marine conditions the relatively low density of the interstitial fluid in a hyperpycnal flow may lead to convection from the upper surface of the flow and lofting of the head. In contrast, because surge-like flows are generated within the marine basin lofting is less likely (although it may occur in stratified basins; cf. Rimoldi et al., 1996).

At a given location velocity increases abruptly as the head of a surge-like flow arrives (rapid waxing) and then generally decreases during the passage of the body and tail (waning flow) (Kneller and Buckee, 2000) thus surge-like flows are typically unsteady. Following the arrival of the front of a quasi-steady current, velocity may remain constant (or nearly so), increase or fluctuate for a prolonged period, before finally waning when the runoff stops or suspended sediment concentration falls below the critical value. Consequently coarsening-up units are far more likely to occur in hyperpycnal turbidites (hyperpycnites; Mulder et al., 2002) than in classic turbidites, and deposits may have fairly uniform character for significant thickness.

Both quasi-steady and surge-like turbidity flows may be locally accumulative, uniform, or depletive (Kneller, 1995) depending on the bed topography and entrainment of both sediment and water. However, the shapes of flood hydrographs vary greatly as does the suspended sediment flux and consequently hyperpycnal flow behaviour and deposits may be more variable than surge-like flows.

Hyperpycnal flow can be maintained over relatively long time periods, allowing significant amounts of deposition from flows that may be relatively dilute. For example, Syvitski and Schafer (1996) and Mulder et al. (1998) related a 10 m thick turbidite in the Saguenay Fjord (Canada) to an 11 day flow event. In surge and surge-like turbidity flows the behaviour of the head of the flow is of major importance as processes operating within the head have a major influence on a large proportion of the deposits. In contrast, in hyperpycnal turbidity currents the behaviour of the flow head is of minor importance as most of the deposit is formed long after the flow front has passed and most deposition (and erosion) is controlled by processes within the body of the flow (Mulder and Alexander, 2001a). Although hyperpycnal turbidity currents are generally less concentrated and therefore slower than surge-like turbidity flows generated from slope failure (see Skene et al., 1997; Mulder et al., 1998) they might cause more substantial erosion, transport and deposition because of their duration.

5. Conclusions

In our experiments the thickness of the flow near the flow front varied with distance from the source depending on slope, effluent discharge, grain size and sorting. Runout distance varied with the proportion of fine-grained sediment rather than with mean grain size. Flow front velocity varied with effluent discharge and sediment concentration and in a complex manner with grain size and sorting. The variation of deposit mass with distance depends on proximal slope angle. The maximum mass per unit area (approximating to maximum bed thickness) is inversely dependent on slope angle. Variation in initial suspended particle concentration resulted in deposits of similar shape but different amplitude. The total mass of the deposit depends directly on the discharge. The amplitude of the peak mass, how-

ever, does not. The distance over which particles are deposited increases and the deposit flattens as particles are deposited progressively further downstream at higher discharges, perhaps relating to more efficient turbulent suspension at higher *Re* (more complete energy cascade), in addition to a longer horizontal component of settling trajectory at higher velocity. The amplitude of the mass peak depended on the grain size. The finer the sediment the more efficient the sediment transport, similar to observations of laboratory surges (Gladstone et al., 1998).

The laboratory results have major implications for interpretation of turbidite sequences. But because of the problems with scaling, additional experiments are needed with bigger experimental configurations and additional data from in situ measurements would be particularly valuable.

Acknowledgements

Thanks to Kate Habgood, Jason Hilton, Gareth Jenkins, Paul Knutz, Sarah Lee, Steve Morris, Damon O'Brien, Viv Ratter, Nicola Rimmington, John Roberts, Steve Shayler, Toby Stewart and Gaelle Yaouancq for help with laboratory experiments. Thanks to Laurence Badham, Claire Bisault and Julie Herniman for technical assistance. Our particular thanks to J. Best, W.R. Normark, J.D. Parsons and K.I. Skene for extensive constructive comments on early versions of this paper.

Appendix

α	bed slope
C_0	suspended sediment concentration in the feed pipe
C_s	suspended sediment concentration
Fr	Froude number
g	acceleration due to gravity
H	thickness of the flow
h_b	the height of the body of the flow
μ	apparent kinematic viscosity
Q	discharge at a given location
Q_0	discharge in the feed pipe
Re	Reynolds number
Ri	Richardson number
Ri_g	'local-gradient' Richardson number
ρ_f	the bulk density of the flow
ρ_a	the density of the ambient water
V	the mean forward velocity
V_x	flow velocity at distance x
x	distance from the pipe outlet

References

Alexander, J., 1993. A discussion on the use of analogues for reservoir geology. In: Ashton, M. (Ed.), Advances in Reservoir Geology. Geol. Soc. London Spec. Publ. 69, 175–194.

Bornhold, B.D., Ren, P., Prior, D.B., 1994. High-frequency turbidity currents in British Columbia fjords. Geo-Mar. Lett. 14, 238–243.

Chikita, K., 1990. Sedimentation by river-induced turbidity currents: field measurements and interpretations. Sedimentology 37, 891–905.

De Rooij, F., Dalziel, S.B., 2001. Time- and space-resolved measurements of deposition under turbidity currents. In: McCaffrey, W.D., Kneller, B.C., Peakall, J. (Eds.), Particulate Gravity Currents. Int. Assoc. Sedimentol. Spec. Publ. 31, 207–215.

Edwards, D.A., 1993. Turbidity Currents: Dynamics, Deposits and Reversals. Lecture Notes in Earth Sciences 44. Springer, Berlin, 173 pp.

Ellison, T.H., Turner, S.J., 1959. Turbulent entrainment in stratified flows. J. Fluid Mech. 6, 432–447.

Forel, F.A., 1885. Les ravins sous-lacustres des fleuves glaciaires. C. R. Acad. Sci. Paris 101, 725–728.

Forel, F.A., 1892. Le Léman: Monographie Limnologique, Vol. 1, Géographie, Hydrographie, Géologie, Climatologie, Hydrologie. Rouge, Lausanne, 543 pp.

Fukushima, Y., Parker, G.A., Pantin, H.M., 1985. Prediction of the ignitive turbidity currents in Scripps Submarine Canyon. Mar. Geol. 67, 55–81.

Garcia, M.H., 1993. Hydraulic jumps in sediment-driven bottom currents. J. Hydraul. Eng. 119, 1094–1117.

Gennesseaux, M., Guibout, P., Lacombe, H., 1971. Enregistrement de courants de turbidité dans la vallée sous-marine du Var (Alpes-Maritimes). C. R. Acad. Sci. Paris Ser. D 273, 2456–2459.

Gladstone, C., Phillips, J.C., Sparks, R.S.J., 1998. Experiments on bidisperse, constant-volume gravity currents: propagation and sediment deposition. Sedimentology 45, 833–843.

Hay, A.E., 1987. Turbidity currents and submarine channel formation in Rupert Inlet, British Columbia, 2. The roles of continuous and surge-type flow. J. Geophys. Res. 92, 2883–2900.

Huppert, H.E., Simpson, J.E., 1980. The slumping of gravity currents. J. Fluid Mech. 99, 785–799.

Imran, J., Parker, G., Katopodes, N., 1998. A numerical model of channel inception on submarine fans. J. Geophys. Res. 103, 1219–1238.

Kineke, G.C., Woolfe, K.J., Kuehl, S.A., Milliman, J., Dellapenna, T.M., Purdon, R.G., 2000. Sediment export from the Sepik River, Papua New Guinea: evidence for a divergent sediment plume. Cont. Shelf Res. 20, 2239–2266.

Kneller, B.C., 1995. Beyond the turbidite paradigm: physical models for deposition of turbidites and their implications for reservoir prediction. In: Hartley, A.J., Prosser, D.J. (Eds.), Characterization of Deep Marine Clastic Systems. Geol. Soc. London Spec. Publ. 94, 31–49.

Kneller, B.C., Buckee, C., 2000. The structure and fluid mechanics of turbidity currents: a review of some recent studies and their geological implications. Sedimentology 57 (Suppl. 1), 62–94.

Laurent, R., 1971. Charge Solide en Suspension et Géochimie dans un Fleuve Côtier Méditerranéen, Le Var (Alpes-Maritimes). PhD Thesis, Université de Nice, Nice, 249 pp.

Laval, A., Cremer, M., Beghin, P., Ravenne, C., 1988. Density surges: two-dimensional experiments. Sedimentology 35, 73–84.

Middleton, G.V., 1966. Experiments on density and turbidity currents. I. Motion of the head. Can. J. Earth Sci. 3, 523–546.

Middleton, G.V., 1967. Experiments on density and turbidity currents. III. Deposition of sediment. Can. J. Earth Sci. 4, 475–505.

Middleton, G.V., 1993. Sediment deposition from turbidity currents. Annu. Rev. Earth Planet. Sci. 21, 89–114.

Morris, S.A., Kenyon, N.H., Limonov, A.F., Alexander, J., 1998. Downstream changes of large-scale bedforms in turbidites around the Valencia Channel Mouth, Northwest Mediterranean: implications for paleoflow reconstruction. Sedimentology 45, 365–377.

Mulder, T., Alexander, J., 2001a. The physical character of subaqueous sedimentary density currents and their deposits. Sedimentology 48, 269–299.

Mulder, T., Alexander, J., 2001b. Deposit thickness variations caused by abrupt change in slope in concentrated particle-driven density currents. Mar. Geol. 175, 221–235.

Mulder, T., Syvitski, J.P.M., 1995. Turbidity currents generated at river mouths during exceptional discharges to the world oceans. J. Geol. 103, 285–299.

Mulder, T., Syvitski, J.P.M., 1996. Climatic and morphologic relationships of rivers: implications of sea level fluctuations on river loads. J. Geol. 104, 509–523.

Mulder, T., Savoye, B., Syvitski, J.P.M., Cochonat, P., 1996. Origine des courants de turbidité enregistrés à l'embouchure du Var en 1971. C. R. Acad. Sci. Paris Sér. IIa 322, 301–307.

Mulder, T., Syvitski, J.P.M., Skene, K.I., 1998. Modelling of erosion and deposition by turbidity currents generated at river mouths. J. Sediment. Res. 68, 124–137.

Mulder, T., Migeon, S., Savoye, B., Faugères, J.-C., 2001a. Inversely-graded turbidite sequences in the deep Mediterranean. A record of deposits by flood-generated turbidity currents? Geo-Mar. Lett. 21(2), 86–93.

Mulder, T., Migeon, S., Savoye, B., Jouanneau, J.-M., 2001b. Twentieth century floods recorded in the deep Mediterranean sediments. Geology 29, 1011–1014.

Mulder, T., Migeon, S., Savoye, B., Faugères, J.-C., 2002. Inversely-graded turbidite sequences in the deep Mediterranean. A record of deposits by flood-generated turbidity currents? A reply. Geo-Mar. Lett. 22, in press.

Nemec, W., 1995. The dynamics of deltaic suspension plumes. In: Oti, M.N., Postma, G. (Eds.), Geology of Deltas. Balkema, Rotterdam, pp. 31–93.

Normark, W.R., 1989. Observed parameters for turbidity current flow in channels, Reserve Fan, Lake Superior. J. Sediment. Petrol. 59, 423–431.

Parker, G.A., Fukushima, Y., Pantin, H.M., 1986. Self-acceleration turbidity currents. J. Fluid Mech. 171, 145–181.

Parsons, J.D., Garcia, M.H., 1998. Similarity of gravity current fronts. Phys. Fluids 10, 3209–3213.

Parsons, J.D., Bush, J.W.M., Syvitski, J.P.M., 2001. Hyperpycnal plume formation from riverine outflows with small sediment concentrations. Sedimentology 48, 465–478.

Phillip, A.C., Smith, N.D., 1992. Delta slope processes and turbidity currents in prodeltaic submarine channels, Queen inlet, Glacier Bay, Alaska. Can. J. Earth Sci. 29, 93–101.

Piper, D.J.W., Savoye, B., 1993. Processes of late Quaternary turbidity current flow and deposition on the Var deep-sea fan, north-west Mediterranean Sea. Sedimentology 40, 557–582.

Piper, D.J.W., Hiscott, R.N., Normark, W.R., 1999. Outcrop-scale acoustic facies analysis and latest Quaternary development of Hueneme and Dume submarine fans, offshore California. Sedimentology 46, 47–78.

Ravenne, C., Beghin, P., 1983. Apport des expériences en canal à l'interprétation sédimentologique des dépôts de cônes détriques sous-marines. Rev. Inst. Fr. Pétrol. 38, 279–297.

Rimoldi, B., Alexander, J., Morris, S.A., 1996. Experimental turbidity currents entering density-stratified water: analogues for turbidites in Mediterranean hypersaline basins. Sedimentology 43, 527–540.

Russell, A.J., Knudsen, Ó., 1999. Controls on sedimentology of the November 1996 jökulhlaup deposits, Skeidarársandur, Iceland. In: Smith, N.D., Rogers, J. (Eds.), Fluvial Sedimentology VI. Int. Assoc. Sedimentol. Spec. Publ. 28, 315–329.

Simpson, J.E., 1987. Gravity Currents in the Environment and the Laboratory. Halsted, Chichester, 244 pp.

Skene, K.I., Mulder, T., Syvitski, J.P.M., 1997. INFLO1: A model predicting the behaviour of turbidity currents generated at river mouths. Comput. Geosci. 23, 975–991.

Sparks, R.S.J., Bonnecaze, R.T., Huppert, H.E., Lister, J.R., Hallworth, M.A., Madder, H., Phillips, J., 1993. Sediment-laden gravity currents with reversing buoyancy. Earth Planet. Sci. Lett. 114, 243–257.

Syvitski, J.P.M., Schafer, C.T., 1996. Evidence for an earthquake-triggered basin collapse in Saguenay Fjord, Canada. Sediment. Geol. 104, 127–153.

Wright, L.D., 1977. Sediment transport and deposition at river mouth: a synthesis. Geol. Soc. Am. Bull. 88, 857–868.

Xu, J., 1999. Grain-size characteristics of suspended sediment in the Yellow River, China. Catena 38, 243–263.